

Highlights

Reducing RES Droughts through the integration of wind and Solar PV

Boris Morin, Aina Maimó Far, Damian Flynn, Conor Sweeney

- RES droughts are analysed using 45 years of hourly wind and solar PV generation data
- RES droughts from C3S-Energy and ERA5-Atlite datasets are compared
- Adding solar PV to a wind-dominated system reduces RES drought frequency and duration
- Validated RES datasets are crucial to accurately identify RES drought extremes

Reducing RES Droughts through the integration of wind and Solar PV

Boris Morin^{a,*}, Aina Maimó Far^a, Damian Flynn^b, Conor Sweeney^a

*^aSchool of Mathematics and Statistics, University College Dublin, Belfield, Dublin
4, Dublin, D04 V1W8, Ireland*

*^bSchool of Electrical and Electronic Engineering, University College Dublin, Belfield,
Dublin 4, Dublin, D04 V1W8, Ireland*

*Corresponding author

Email addresses: `boris.morin@ucdconnect.ie` (Boris Morin),
`aina.maimofar@ucd.ie` (Aina Maimó Far), `damian.flynn@ucd.ie` (Damian Flynn),
`conor.sweeney@ucd.ie` (Conor Sweeney)

Abstract

Increasing the share of electricity produced from renewable energy sources (RES), combined with RES dependence on weather, poses a critical challenge for energy systems. This study investigates the importance of the balance between wind and solar photovoltaic (PV) capacity on periods of low renewable generation, known as RES droughts. Three different RES models are used to estimate the capacity factors for different scenarios of installed capacities for wind and solar PV power. The skill of the RES models is quantified by comparing capacity factor time series to observed hourly data and by assessing their representation of observed RES droughts. The RES models are used to generate a 45-year hourly time series of RES capacity factor, enabling analysis of the frequency, duration and return periods of RES droughts at a climatological scale. Results show the importance of using an accurate, validated RES model for RES drought risk assessment. The addition of solar PV capacity to a wind-dominated system results in a significant reduction in the frequency and duration of RES droughts, while also reducing extremes and seasonal drought patterns. These findings underscore the importance of diversification in RES capacity to enhance energy security and resilience.

Keywords: RES Drought, Wind Power, Solar PV Power, Renewable Energy Sources, Return Periods

1. Introduction

The EU aims to generate at least 69% of its electricity from renewable energy sources (RES) by 2030, up from 41% in 2022 [1]. While this transition is essential for reducing greenhouse gas emissions, it also highlights the challenge of managing the variability of weather-dependent energy sources such as wind and solar photovoltaic (PV) power. This challenge is amplified by the increasing electrification of energy sectors, which places greater demand on the power system and makes it more sensitive to meteorological conditions, both in historical [2] and future climates [3]. Periods of low renewable generation, known as *Dunkelflaute* or RES droughts, pose significant risks to system adequacy and energy security, emphasising the need for a resilient energy system to meet both growing electricity demand and decarbonisation targets.

RES drought events do not have a fixed definition, with various approaches present in the literature. One common method defines a RES drought as a period during which the average capacity factor (CF) remains below a fixed threshold for a specified duration. For example, Kaspar et al. [4] used this method to investigate the shortfall risks of low wind and solar PV generation in Europe, with a focus on Germany, testing multiple CF thresholds and durations. Similarly, Mockert et al. [5] examined the link between weather regimes and RES droughts in Germany using a 48-hour rolling window under a threshold to define RES droughts. Similar fixed-threshold approaches have also been applied using CF series reconstructed through machine learning in regions such as Japan [6] and Hungary [7].

Alternative methods adjust the CF threshold dynamically over the year to account for seasonal variations in renewable production. Raynaud et al. [8] defined droughts as sequences of days with energy production below a threshold that varies seasonally, a methodology later adapted for India [9]. Building on this, Kapica et al. [10] compared the likelihood of increased RES droughts in Europe under different climate models. Other studies have defined droughts based on deviations from daily mean production: Rinaldi et al. [11] applied these in the U.S. Western Interconnection to quantify the benefits of long-term storage, while Brown et al. [12] examined weekly timescales to explore meteorological influences on the most severe drought events. Another method defines energy drought indices based on metrics commonly used in hydro-meteorology to characterise RES droughts [13]. This approach identifies periods of unusually low generation relative to historical production levels, using the lowest production percentiles. Bracken et al. [14] used this approach to analyse RES droughts at different time scales in the U.S. [14], and Lei et al. [15] used it to quantify droughts in wind-PV-hydro systems in China.

In addition to examining periods of low renewable electricity generation, several studies also explore the periods when the imbalance between renewable generation and electricity demand (residual load) is high. Raynaud et al. [8] defined both energy production and energy supply droughts, and showed the difference in their patterns in a hypothetical fully renewable system composed of wind, PV and run-of-the-river hydropower. Similarly, Allen and Otero [13] also defined a standardised index based on meteorological droughts to address residual load, whose correlation to the energy production index is mostly negative (as expected, although quite low anticorrelations and even small positive correlations appear for some European countries). This

index was also applied to the U.S. by Bracken et al [14], revealing a consistent increase in the drought magnitude when load is considered, despite showing differing results across regions.

In this paper, the focus is exclusively on renewable electricity generation, which allows us to maintain physical models that do not consider the behavioural influence of demand, whose role will be addressed in the discussion. A fixed threshold approach is used to define RES droughts, which facilitates consistent inter-comparison between scenarios with different installed wind and solar PV capacities. The case study used in this paper is Ireland, a region with a strong reliance on wind power and ambitious targets for solar PV power expansion. This provides valuable insights into the potential benefits of diversifying the renewable energy mix on RES droughts in the context of realistic scenarios.

RES droughts are identified using onshore wind and solar PV CF time series. In this study, three different datasets are used and compared, all of which are driven by the ERA5 reanalysis [16]. Two of the datasets are part of C3S Energy (C3S-E), an energy-based operational dataset produced by the EU Copernicus Climate Change Service [17]. One of the C3S-E datasets provides CF time series aggregated at the national scale, while the other provides the CF time series at each grid point, at the ERA5 resolution of 0.25° . The third dataset was generated using the Atlite model [18], which converts the ERA5 atmospheric data to a generation time series using specified wind turbine and PV panel models. Atlite is an open-source tool developed by PyPSA [18] and has been used for estimating wind and solar PV generation in order to study RES droughts [5].

Generic datasets for wind and solar PV CF are often used for the quantification of RES droughts. Despite most of them undergoing a validation process, they are often not fully representative of all geographical locations, and even show strong differences between each other [19]. In this work, we quantify the skill of a generic model for Ireland (a region not commonly used for generic model validation), and explore the effect that using it has on RES droughts when compared to a specifically-designed model. This comparison is propagated through the whole analysis to fully see the effect of these differences in the context of a transition from a wind-only system to a more balanced mix that includes solar PV. In terms of the drought definition, the literature often uses daily averaged values, which limits the start and end times of events. We opt for a 24-hour rolling average, which avoids potential masking of day-long events due to their start time.

Therefore, the aim of this study is to answer three questions which could help on the decision making for the planning of reserve capacity in real case wind-dominated renewable energy system:

- Can generic datasets be used to quantify extreme events like RES droughts?
- What is the impact of modelling assumptions on the analysis of RES droughts?
- How does the integration of solar PV into a predominantly wind-based system alter the characteristics of RES droughts in a real-case setting?

The datasets used in this study are detailed in section 2, which describes their characteristics and relevance for evaluating RES droughts. Section 3 outlines the RES datasets used to simulate wind and solar PV generation and provides the methodology for defining and identifying RES drought events, including the thresholds and metrics applied. In section 4, the datasets are first verified against observed energy data to assess their accuracy, followed by an analysis of RES drought occurrences for two scenarios with different ratios of installed wind to solar PV capacities. Finally, section 5 offers a discussion of the results in the context of energy reliability and future planning, followed by the main conclusions and recommendations for further research.

2. Data

This study uses publicly available datasets to construct and validate the datasets for estimating the CF of wind and solar PV power. The primary data sources include: EirGrid and SONI, the transmission system operators (TSO) for the Republic of Ireland and Northern Ireland, respectively; the ERA5 reanalysis dataset; and the C3S-E datasets.

2.1. Wind and solar PV Capacity and Availability

EirGrid, the TSO for the Republic of Ireland, and SONI, the Northern Ireland TSO, provide detailed datasets on all wind and solar PV farms across the island of Ireland (Republic of Ireland and Northern Ireland) from 1990 to the present [20]. These datasets include information such as each farm's installed capacity, name, and connection date. To enhance the accuracy of this data, the longitude and latitude for each farm were manually determined

122 through online searches. For simplicity, this data will be referred to as orig-
 123 inating from EirGrid, as all-island data was directly obtained from EirGrid,
 124 and the combined regions of the Republic of Ireland and Northern Ireland
 125 will be referred to as Ireland throughout the remainder of this document.

126 The spreadsheet available from the EirGrid website contains two key vari-
 127 ables: generation and availability. Generation is the energy that a RES farm
 128 actually contributed to the grid, which may include limitations introduced
 129 by the TSO to maintain grid stability, such as constraints and curtailment.
 130 Availability represents the energy that would have been generated from a RES
 131 farm if no grid constraints had been applied, making it representative of the
 132 weather-related response. Generation and availability values are available
 133 from 2014 onward for wind power and from 2018 onward for solar PV power,
 134 although solar PV availability data only became present in the Republic of
 135 Ireland in 2023. This study focuses on availability for all analyses.

136 2.2. Atmospheric Variables

137 Atlite and C3S-E datasets are driven by the ERA5 reanalysis [16], pro-
 138 duced by the European Centre for Medium-Range Weather Forecasts (ECMWF).
 139 This global gridded dataset provides hourly atmospheric variables from 1940
 140 to the present at a horizontal resolution of 0.25°. It has proven to be the best
 141 choice for studying renewable energy in Ireland [21]. Table 1 lists the ERA5
 142 variables used by Atlite and C3S-Energy.

Table 1: ERA5 variables used to calculate wind and solar PV generation

ERA5 name	variable
100 metre zonal and meridional wind speed	u_{100}, v_{100}
2 metre temperature	$t2m$
Surface net solar radiation	ssr
Surface solar radiation downwards	$ssrd$
Top of atmosphere incident radiation	$tisr$
Total sky direct solar radiation at surface	$fdir$

143 2.3. C3S Energy

144 The EU Copernicus Climate Change Service developed the C3S-E renew-
 145 able energy dataset for Europe [17], using ERA5 atmospheric variables and
 146 weather-to-energy models. This dataset provides hourly CF for wind and

147 solar PV energy from 1979 to the present. The data are available on the
 148 same grid as the ERA5 data, which has a horizontal resolution of 0.25° . The
 149 time series are also available for download at two aggregated scales: regional
 150 (NUTS 2) and national.

151 The wind CF in the C3S-E model is calculated using wind speeds at 100
 152 metres (u_{100} , v_{100}) and a standard turbine model, the Vestas V136/3450,
 153 with a fixed hub height of 100 meters. This choice reflects trends in wind
 154 turbine installations and was guided by expert recommendations. Since real-
 155 time data on the exact wind turbine fleet across Europe is difficult to obtain,
 156 C3S-E assumes a homogeneous distribution of turbines across the ERA5 grid.
 157 While this approach does not capture the precise capacity factors reported
 158 by grid operators, it provides a well-correlated time series that effectively
 159 represents the impact of climate variability on wind power generation. The
 160 turbine power curves used in the model are sourced from publicly available
 161 databases, ensuring consistency with industry standards. The solar PV CF
 162 in the C3S-E model is calculated at the grid level and represents the aggre-
 163 gated output of all solar PV systems within each pixel, rather than a single
 164 installation. It is derived from meteorological data, including surface solar
 165 radiation downwards ($ssrd$) and air temperature ($t2m$), using a reference
 166 solar PV plant model. This model incorporates empirical calculations for
 167 key system components such as optical losses, module efficiency, and invert-
 168 ers. The final CF accounts for a mix of module orientations typical for each
 169 location [22].

170 3. Methods

171 This study uses onshore wind and solar PV CF time series from three
 172 datasets to analyse RES droughts across the island of Ireland. Data down-
 173 loaded from C3S-E were used to obtain two datasets: one based on national-
 174 level data (C3S-E N), and another on grid-level data (C3S-E G). The third
 175 dataset was computed using the Atlite model (Atlite).

176 3.1. C3S-Energy National: C3S NAT

177 The C3S NAT dataset is created by combining different national and
 178 regional data sources. The inputs used are the total installed capacity in
 179 the Republic of Ireland and Northern Ireland, and the aggregated CF time
 180 series provided by C3S-E at the two corresponding NUTS levels: Republic of
 181 Ireland (NUTS0: IE) and Northern Ireland (NUTS2: UKN0). These values

are based on the assumption that RES generation occurs at every ERA5 grid point in Ireland. To get the C3S NAT CF for all of Ireland, a weighted average of the two obtained CF time series is performed, using the actual installed capacity as weights.

3.2. C3S-Energy Gridded: C3S GRID

The C3S GRID dataset combines information that contains the spatial variability over Ireland. The inputs used to create this dataset consist of the CF time series from C3S-E over the ERA5 grid, along with the location and characteristics of individual RES farms across Ireland, as explained in section 2.1. For each farm, the nearest grid point on the C3S-E dataset was identified, the generation from that farm was calculated using the retrieved CF from C3S-Energy, and it was added to a total generation. This total generation was divided by the total installed capacity to convert it back to CF. This is equivalent to performing a weighted average of the CF associated with each farm using the farm’s installed capacities as weights. The C3S GRID dataset contains the resulting CF time series, which accounts for the actual spatial distribution of wind and solar PV farms in Ireland.

3.3. Atlite: ATLITE

The ATLITE dataset is constructed by using the Atlite model to process weather variables into energy variables. This model allows for a tuning process where the models used to transform wind and solar PV can be adjusted to best represent the observed data up until this point for the relevant region (in this case, Ireland). The Atlite model takes as inputs the locations of RES farms and ERA5 weather variables: wind speed at 100 metres (u_{100} , v_{100}) for wind generation, and radiation variables (ssr , $ssrd$, $tisr$, and $fdir$) along with air temperature ($t2m$) for solar PV generation. These meteorological inputs are processed using the Atlite model to estimate CF time series for wind and solar PV, incorporating specific characteristics such as the wind turbine power curve and PV panel model selected for this specific case. The output of the Atlite model is a generation time series, which divided by the total capacity to transform it back into CF, which is what we call the ATLITE dataset. The flexibility in the usage of different power curves and PV panel models represents the key distinction between this dataset and the two C3S-derived ones. This study identifies the most appropriate wind turbine power curve to use from the 121 power curves at five different levels of smoothing made available by Renewables.ninja [23], and selects the PV panel model out

of the options available within the Atlite model. The selection of a specific wind turbine and PV panel characteristics is further discussed and explained in section 4.1.

3.4. Energy Scenarios

The output of those three datasets are one CF time series for both wind and Solar PV. In addition to analysing wind and solar PV generation separately, a combined CF was computed for each dataset by averaging wind and solar PV generation, weighted by their installed capacities at the end of 2023 (5.9 GW for wind power and 0.6 GW for solar PV power). This configuration is referred to as the 91W-9PV scenario, reflecting the distribution of 91% wind and 9% PV capacity. Given that solar PV capacity in Ireland is low in 2023, and to explore how a more balanced distribution of wind and solar PV capacities might impact RES droughts, this study also considered a second scenario, referred to as 57W-43PV, where the installed solar PV capacity is assumed to increase to 8.6 GW, while wind capacity rises to 11.45 GW. These values are based on targets outlined in the roadmap published by the 2024 Climate Action Plan [24]. This study does not include offshore wind in the analysis. Recent reports suggest that even by 2030, Ireland is unlikely to have any significant new offshore wind farms, with projected offshore capacity expected to remain near zero using realistic scenarios [25].

New time series were generated for both the Atlite and C3S-E G solar PV datasets, incorporating a revised distribution of installed capacity across Ireland as specified in the roadmap. For wind power, the CF time series remains unchanged, as significant shifts in the location of wind farms are not expected. In total, twelve CF time series were analysed in this study, six for individual wind and solar PV CF (three datasets for each source) in the 91W-9PV scenario, and an additional six time series that include the combined CF for 91W-9PV and 57W-43PV scenarios across the different datasets.

It is important to note that the specific capacity values used in this study are illustrative and are not intended to reflect precise future realities. Instead, they serve to explore the impact of transitioning from a wind-dominated system (91W-9PV) to a more evenly distributed system (57W-43PV). This approach allows for a comparative analysis between the two scenarios, assessing how the balance of RES capacity affects the occurrence of RES droughts.

For each dataset (Atlite, C3S-E G, and C3S-E N), four distinct scenarios are examined, as summarised below:

- Wind Power - based on the actual capacity at the end of 2023
- Solar PV Power - based on the actual capacity at the end of 2023
- Combined RES / 91W-9PV - based on the actual capacity at the end of 2023
- Combined RES / 57W-43PV - based on the capacity projected for 2030

3.5. RES Drought Definition

In this study, a RES drought event was defined as occurring when the 24-hour moving average of CF remains below a fixed threshold of 0.1 for a period of longer than 24 hours. The choice of this threshold is somewhat arbitrary, but aligns with similar studies on low renewable energy production [4, 6, 7]. By using a 24-hour moving average, fewer but longer-lasting events were captured compared to using the raw CF time series, which can be more sensitive to short-term fluctuations. A fixed threshold approach was chosen in this study to enable consistent inter-comparison between datasets.

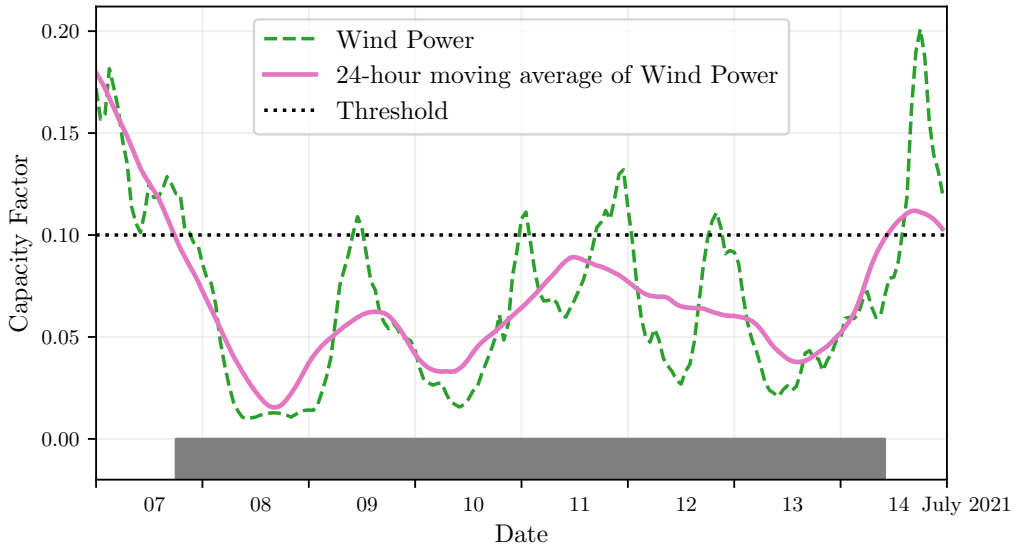


Figure 1: Wind time series of CF (green) and its 24-hour moving average (pink) from the 7th to the 15th of July 2021. The black dashed line indicates the CF threshold. The grey bar shows the period identified as a wind drought under our definition

268 The moving average approach smooths out short-term fluctuations, so
 269 that brief periods above the threshold do not interrupt an otherwise con-
 270 tinuous low-CF period (Fig. 1). This means that a single hour above the
 271 threshold does not "break" a drought event if it is surrounded by prolonged
 272 low-generation hours. As a result, fewer but longer-lasting drought events
 273 are identified, which may better reflect real-world conditions where energy
 274 supply constraints persist over extended periods.

275 4. Results

276 4.1. Verification

277 The accuracy of the datasets used in this study was verified, before con-
 278 tinuing to the analysis of RES droughts. For the verification process, time-
 279 varying values of installed capacity were used to account for changes in RES
 280 development over the verification period. This step allowed us to assess how
 281 well the datasets represent the production of renewable energy by comparing
 282 them against observed data.

283 4.1.1. Wind Energy

284 The C3S-E datasets use the Vestas V136/3450 wind turbine power curve,
 285 (Fig. 2a). The Atlite model allows the user to specify the power curve.
 286 We considered the 121 power curves available for download from Renew-
 287 ables.ninja [23]. For each power curve, Renewables.ninja also provides four
 288 associated smoothed power curves. The smoothing is done using a Gaussian
 289 filter with different standard deviations that depend on the wind speed. A
 290 separate wind CF time series for Ireland was generated for each of the wind
 291 turbine power curves and smoothing levels.

292 The performance of each CF time series is then assessed based on four skill
 293 scores: correlation coefficient (CC), root mean square error (RMSE), mean
 294 bias error (MBE), and the percentage of overlap. The percentage of overlap
 295 quantifies the similarity between the observed and modelled distributions. It
 296 is a positively oriented skill score, where 100% shows full agreement between
 297 the two distributions, and 0% indicates no overlap. The histograms of hourly
 298 CF values for the most recent decade (2014-2023) are used to calculate this
 299 skill score.

300 Based on these metrics, the most representative power curve for Ireland
 301 is the Enercon E112.4500 power curve with the $0.3w$ smoothing filter. The
 302 smoothing of the wind turbine power curve represents losses associated with

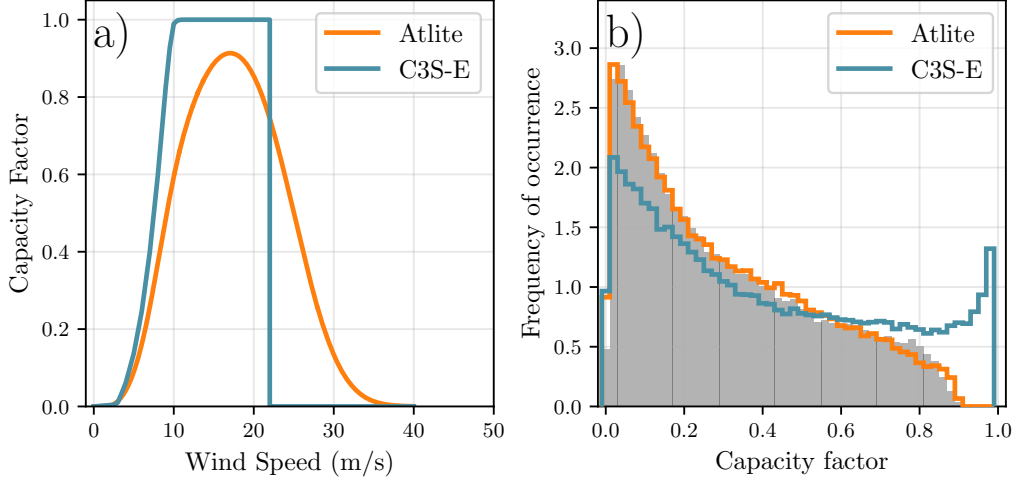


Figure 2: a) Power curves of the Enercon E112.4500 with a 0.3w smoothing filter used by Atlite (orange) and the Vestas V136/3450 used by C3S-E (blue) b) Histograms of wind CF for Ireland from Atlite (orange), C3S-E (blue) and Observed (shaded)

each turbine, as well as losses such as wake effects between turbines, which are important when modelling wind energy on larger spatial scales. The histogram in Fig. 2b shows that the C3S-E power curve tends to underestimate low CF values and overestimate higher ones, whereas the smoothed Atlite power curve more closely follows the observed wind availability data. This is further supported by the percentage of overlap which is higher for Atlite (97.2%) than for C3S-E (83.2%), indicating better agreement with observed data.

The effect of the difference between the power curves is also visible in Fig. 3, which shows a density plot of wind CF values. The two C3S-E datasets are shown to overestimate the observed CF, whereas the Atlite model is in good agreement with the observed data. The skill scores presented in Table 2 show that Atlite performs better than the C3S-E datasets for all of the skill scores.

Fig. 4 shows the average annual number of wind drought events during the 2014 to 2023 validation period. The figure reveals that Atlite presents the best overall agreement with the observed frequency and duration of wind drought events. This pattern is particularly evident for shorter-duration events, which are the most frequent.

The verification of wind generation has put forward two main facts. On

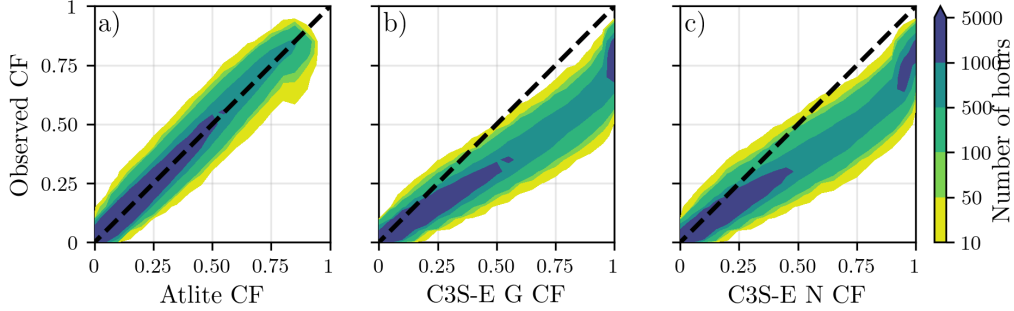


Figure 3: Wind CF density plot of the observed CF (vertical axes) and modelled (horizontal axes) CF data for the a) Atlite, b) C3S-E G and c) C3S-E N datasets

	Atlite	C3S-E G	C3S-E N
CC	0.981	0.972	0.970
RMSE	0.045	0.177	0.162
MBE	-0.003	0.137	0.121

Table 2: Skill scores for wind power for the three datasets compared to observed data

the one hand, the ATLITE dataset is skilled at reproducing onshore wind CF and droughts over Ireland .On the other hand, the power curve used for both C3S GRID and C3S NAT is not representative for Ireland, as it severely overestimates generation, underestimating the occurrence of RES droughts. This puts forward one of the problems that come with using generalised datasets for the characterisation of RES droughts: biases severely affect the ability of any given model to reproducing them. The skill scores for the three datasets (Tab. 2) show only a small difference in the ability to reproduce the changes in CF (visible in the very similar CC). However, their ability to reproduce the exact value is much lower than that of ATLITE (RMSE almost 4 times bigger for the two C3S with respect to ATLITE), and particularly biased towards an overestimation of CF (clear in the MBE values), which leads to the underestimation of droughts. This puts forward the need to use fully verified models to assess RES droughts, whose impact on the analysis of RES droughts will be explored in section 4.2.

4.1.2. Solar PV Energy

The Atlite model allows the user to select certain PV panel characteristics. In this study, the three PV panel types available in the Atlite model were

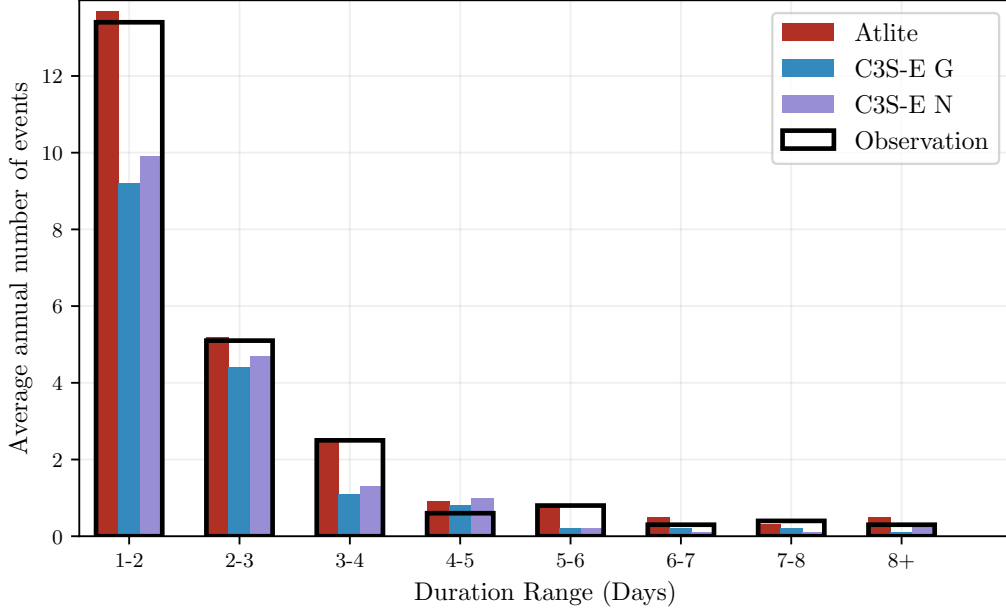


Figure 4: Average annual number of wind drought events for Atlite (red), C3S-E G (blue), C3S-E N (purple), and the observed data (black outline). The wind droughts are identified from 2014 to 2023, considering the actual capacity of the system at any given time

341 considered (CSi, CdTe, Kaneka). Following the same methodology as in the
 342 previous section, the three available models were compared using four skill
 343 scores (CC, RMSE, MBE, and the percentage of overlap). Based on the best-
 344 performing metrics, the Beyer PV panel model was selected [26], using the
 345 Kaneka Hybrid panel option. For all solar PV farm locations, the azimuth
 346 angle is fixed at 180° (due south), and the optimal tilt angle option is applied.

347 The solar PV installed capacity available on the spreadsheets from Eir-
 348 Grid represents the Maximum Export Capacity (MEC) and does not ac-
 349 curately reflect the installed solar PV capacity. To enable actual solar PV
 350 generation potential to be modelled correctly, installed capacities were set at
 351 1.4 times the MEC values. This scaling factor was estimated by analysing
 352 proprietary data from individual solar PV farms provided by EirGrid, which
 353 showed that, on average, assuming that the installed capacities of farms ex-
 354 ceed their MEC values by 40% yields the best agreement with the observed
 355 availability.

356 Figure 5 shows that the three datasets have a similar tendency to overesti-

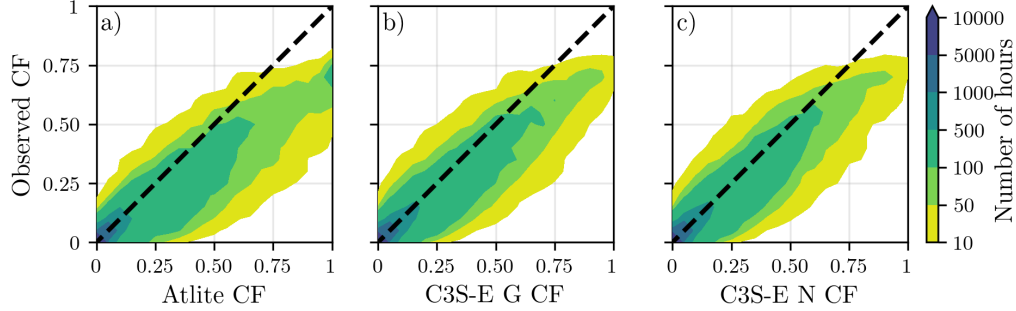


Figure 5: Solar PV CF density plot of the observed (vertical axes) and modelled (horizontal axes) CF series for the a) Atlite, b) C3S-E G and c) C3S-E N datasets

mate the CF compared to the observed values, especially for high CF values. The skill scores presented in Table 3 indicate that C3S-E G performs best overall, with the lowest RMSE and a high correlation coefficient, suggesting a closer match to observed data. All models show a slight positive bias, with Atlite exhibiting a slightly lower correlation and higher RMSE.

	Atlite	C3S-E G	C3S-E N
CC	0.921	0.931	0.931
RMSE	0.119	0.090	0.113
MBE	0.046	0.027	0.021

Table 3: Skill scores for Solar PV CF for the three datasets compared to observed data

Fig. 6 shows the number of solar PV drought events during the 2023 validation period across different duration ranges. The figure reveals partial agreement between the three datasets and the observed data, with consistent results noticed for duration ranges of 1-2, 3-4, 7-8, and 8+ days. However, discrepancies appear in the other ranges, where the models diverge from the observed data. The main challenge in validating solar PV data stems from the recent installation of a large share of Ireland’s solar PV capacity, with over 65% of the total solar PV capacity installed in 2023. This results in uncertainties in solar PV generation data and the actual generating capacity in the first few months after each farm is connected.

As one of the goals of this analysis is to assess the combination of wind and solar PV generation, the complementary nature of these energy sources will mitigate the limitations in solar PV-only results. Still, a few differences

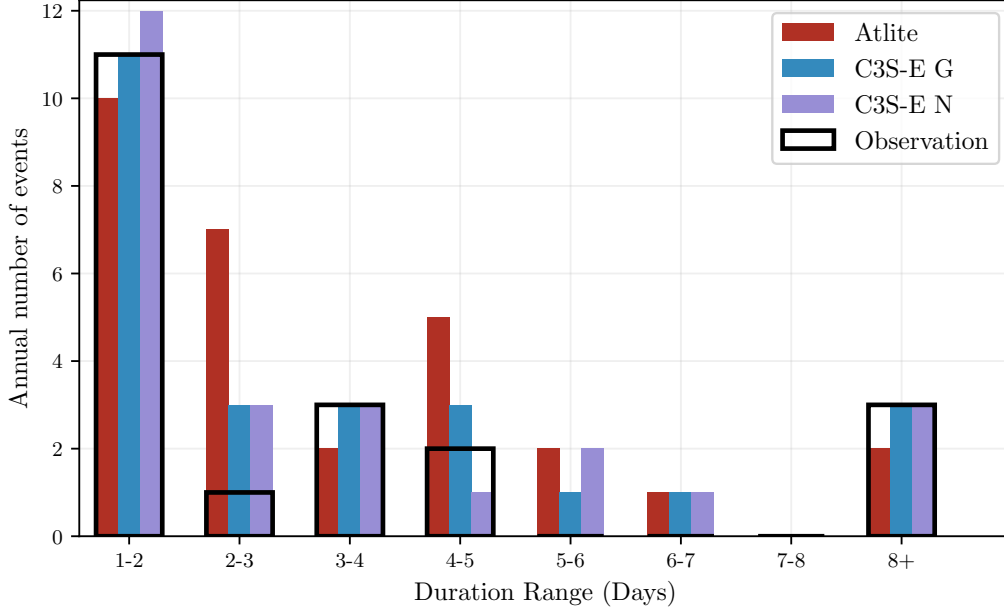


Figure 6: Number of solar PV drought events for Atlite (red), C3S-E G (blue), and C3S-E N (purple) and the observed data (black outline). The solar PV droughts are identified for 2023, considering the actual capacity of the system at any given time

375 between wind and solar PV stand out. First, no single model has proven best
376 for the characterisation of solar PV, although the statistical approach taken
377 by the two C3S datasets has proven superior to the single panel model in
378 ATLITE (Tab. 3). The short time considered in the verification due to the
379 limited data availability for solar PV in Ireland is part of the cause for our
380 limited ability to select a specific overall best solar PV dataset. However, our
381 results seem to indicate that it is possible that the generic datasets perform
382 better for solar PV than for wind, as the variability between the different
383 panel models is smaller in comparison to the existing differences between
384 wind turbine power curves. Therefore, all through section 4.2 the differences
385 between the three models will be highlighted, considering that neither stands
386 out positively.

387 4.2. Analysis

388 In this section, RES drought events are evaluated under two different
389 scenarios with fixed installed capacities: the 91W-9PV scenario, with 5.9

390 GW of wind capacity and 0.6 GW of solar PV capacity; and the 57W-43PV
391 scenario, where wind capacity comprises 11.45 GW and solar PV capacity
392 increases to 8.6 GW. Both scenarios were driven by 45 years of ERA5 data.
393 Using the RES drought identification process described in Section 3.5, wind
394 and solar PV droughts are first analysed separately before presenting the
395 results for combined (wind + solar PV) RES droughts under both scenarios.

396 It is important to highlight that this analysis considers two key aspects:
397 the absolute values that characterise RES droughts, which are crucial for
398 power system planning, and the relative differences observed when comparing
399 the various datasets and energy scenarios described in Section 3.4. This
400 complete analysis puts forward the differences between the datasets, showing
401 the impact of possible misrepresentations of the system on the analysis of
402 RES drought events.

403 *4.2.1. Annual Number of RES Droughts*

404 The analysis of annual RES drought events reveals trends that are largely
405 consistent with earlier studies. When only wind energy is considered (Fig.7a),
406 the number of drought events decreases as the duration range increases, with
407 very few events lasting more than seven days. This pattern aligns with
408 previous research showing that wind droughts tend to be short and frequent.
409 In contrast, for solar PV energy (Fig.7b), drought frequency declines from one
410 to eight days and then slightly increases for longer durations. This behaviour
411 is attributable to Ireland's high-latitude location, where reduced sunlight in
412 winter (from November to March) leads to consistently low solar PV output.

413 Moreover, the comparison between wind and solar PV results indicates
414 that the median, first, and third quartiles for solar PV are consistently higher
415 than or equal to those for wind. This is expected, given that solar PV gen-
416 eration is inherently lower, zero at night, and limited by the solar cycle, as
417 observed in other studies. When wind and solar PV are combined under the
418 91W-9PV scenario (Fig.7c), the results closely mirror those of wind alone,
419 reaffirming wind's dominance in the current energy mix. However, in the
420 57W-43PV scenario (Fig.7d), a marked reduction in drought events is ob-
421 served across all datasets, with a decrease of the total number of events of
422 56% for Atlite, 52% for C3S-E G, and 50% for C3S-E N, demonstrating the
423 beneficial effects of a more balanced energy mix. These findings are in line
424 with earlier studies that highlight how increasing solar PV capacity can miti-
425 gate drought frequency through the anti-correlated seasonal patterns of wind
426 and solar generation.

427 Additionally, the consistently higher drought counts reported by the Atlite
 428 dataset, compared to the C3S-E datasets, underscore the impact of model
 429 selection, particularly the influence of wind turbine power curve represen-
 430 tation, on quantifying RES droughts. This observation is consistent with
 431 previous research, which has also noted that assumptions regarding turbine
 432 characteristics can significantly affect drought duration estimates. Despite
 433 the differences in the number of RES droughts detected by each dataset,
 434 the overall effect of balancing the shares of wind and solar PV is consistent,
 435 independently of the complexity of the dataset used.

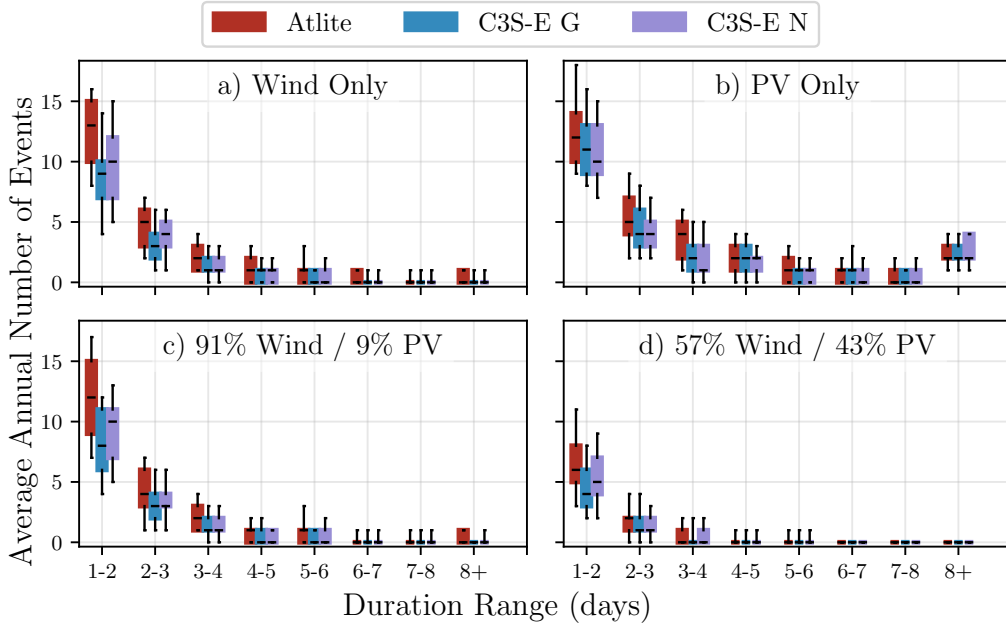


Figure 7: Average annual number of RES droughts (from 1979 to 2023) for a) Wind,
 b) solar PV, c) 91W-9PV and d) 57W-43PV for Atlite (red), C3S-E G (blue), and C3S-E
 N (purple). The x-axis represents duration ranges in days (lower bound included), while
 the y-axis indicates the annual number of events. The boxes display the first and third
 quartiles and the median is marked by a black line. The whiskers indicate the 5th and
 95th percentiles

436 4.2.2. Return Periods of RES Drought Duration

437 The RES drought events identified over the 45-year period were used to
 438 calculate the return periods for different RES drought durations. A return

439 period is the estimated average time interval between events of a specified
 440 duration or intensity (not to be confused with the frequency of their oc-
 441 currence within a fixed time frame). Fig. 8 illustrates the return periods
 442 for varying RES drought durations, highlighting how often different drought
 443 lengths are likely to occur across the datasets. This analysis not only quan-
 444 tifies the likelihood of prolonged low-generation periods but also provides
 445 insight into how extreme events are distributed across different timescales,
 446 helping to assess the variability of rare but impactful events. Understand-
 447 ing these return periods is crucial, as even infrequent droughts can challenge
 448 energy security by placing significant strain on conventional backup sources
 449 necessary to maintain supply in high-RES scenarios.

450 For wind (Fig. 8a), the log-linear increase in return periods observed in
 451 this study confirms that longer droughts occur exponentially less frequently,
 452 a trend consistent with earlier research on wind variability. In the case of so-
 453 lar PV droughts (Fig. 8b), the Atlite dataset shows a general log-linear trend,
 454 whereas the C3S-E datasets exhibit a sudden increase in drought duration
 455 for events exceeding sixteen days. This abrupt rise reflects differences in how
 456 solar PV output is handled near the CF threshold during low irradiance con-
 457 ditions. In the balanced scenario, the reduced share of wind and increased
 458 share of solar PV leverages their complementary seasonal patterns, resulting
 459 in higher return periods for combined drought events. This outcome high-
 460 lights the benefit of a diversified energy mix in enhancing system resilience.

461 Under the 91W-9PV scenario (Fig. 8c), the combined RES drought return
 462 periods largely mirror those for wind alone, reflecting the dominance of wind
 463 in the current energy mix. In contrast, the balanced 57W-43PV scenario
 464 (Fig. 8d) shows a dramatic increase in return periods across all durations,
 465 suggesting that a more diversified energy mix can substantially mitigate the
 466 frequency of prolonged drought events.

467 Across Fig. 8a, c, and, d, the return periods in the Atlite dataset are con-
 468 sistently higher than those in the two C3S-E datasets. For instance, in the
 469 91W-9PV scenario (Fig. 8c), an event with a one-year return period lasts six
 470 days in the Atlite dataset, compared to only five days in the C3S-E datasets.
 471 This difference underscores the importance of model selection when quan-
 472 tifying RES droughts, as each dataset’s assumptions and parametrisations
 473 significantly influence drought duration estimates. Additionally, in all four
 474 graphs, the similarity between results from the two C3S-E datasets suggests
 475 that assumptions in the Atlite dataset, such as wind turbine power curve
 476 selection and PV panel specifications, have a greater impact on RES drought

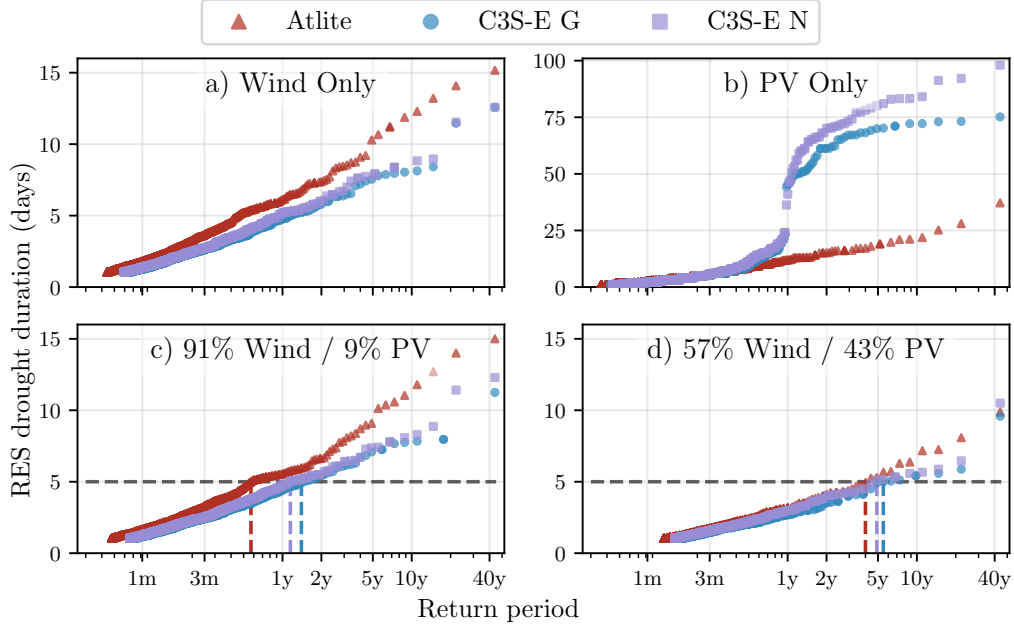


Figure 8: Return periods of the duration of RES droughts (from 1979 to 2023) for a) Wind, b) Solar PV, c) 91W-9PV and d) 57W-43PV for Atlite (red triangle), C3S-E G (blue circle), and C3S-E N (purple square). The x-axis represents the return period time in a log-scale and the y-axis indicates the duration of RES drought associated with it. The horizontal dashed line marks the 5-day return period, with coloured vertical dashed marking its return period for each dataset

477 duration estimates than the precise geographic distribution of RES farms
 478 when studying the return periods of RES droughts.

479 Contrary to the number of events per year and per duration, the return
 480 periods show large differences in the behaviours of the three datasets. The re-
 481 production of average behaviours is still manageable using the C3S datasets,
 482 but the magnitude of extremes is not well reproduced when the share of wind
 483 is large. System planning based on the wrong datasets could yield an under-
 484 estimation of the potential for extreme RES droughts, eventually leading to
 485 shortages linked to undersized reserve capacity. Even though this effect will
 486 be mitigated, affecting only the most extreme events with the introduction
 487 of widespread solar PV, it is important to keep in mind this effect for all
 488 wind-dominated electricity systems.

4.2.3. Seasonal Distribution of RES Droughts

The seasonal analysis of RES droughts is based on the percentage of hours in each month classified as drought events. Wind droughts tend to be more frequent during summer, whereas solar PV droughts are more common in winter due to reduced sunlight. By comparing these seasonal patterns across different datasets and energy scenarios, the study examines how model-specific assumptions and variations in capacity mix affect the overall characterisation of drought events.

For the wind-only scenario (Fig. 9a), the Atlite dataset exhibits a pronounced seasonal pattern, with about 24% of summer hours (June–July–August) identified as droughts compared to only 4% in winter (December–January–February). This strong seasonal signal is less evident in the C3S-E datasets, which suggests that the differences in the underlying wind power curves play a significant role. In Atlite, CF near or below the 0.1 threshold occurs at relatively higher wind speeds, resulting in a higher count of drought hours during the summer months. In contrast, solar PV droughts (Fig. 9b) display an opposite seasonal trend. Across all datasets, over 60% of winter hours are classified as solar PV droughts, reflecting the naturally low solar irradiance in Ireland during winter. Moreover, Atlite tends to record a slightly higher percentage of drought hours for wind and a marginally lower percentage for solar PV relative to the C3S-E datasets. These differences highlight how dataset-specific assumptions, such as the treatment of wind turbine power curves and PV panel characteristics, significantly influences the apparent seasonal dynamics of RES droughts.

The 91W-9PV scenario (Fig. 9c) shows patterns comparable to the ones for wind droughts (Fig. 9a). However, in the 91W/9PV scenario, the number of hours classified as RES droughts in summer decreases slightly compared to the wind-only scenario. This reduction can be explained by the contribution of solar PV generation during the summer months in the 91W-9PV scenario, even though it constitutes only 11% of total capacity. Since the number of RES drought hours for solar PV in summer is near zero, this small contribution has a noticeable impact on reducing overall drought hours. In the 57W-43PV scenario (Fig. 9d), all three datasets show a reduction in monthly RES drought frequency. Annual reductions in median RES drought frequency are observed across the datasets, dropping from 14% to 5% for Atlite, from 8% to 3% for C3S-E G, and from 9% to 4% for C3S-E N. The balanced mix of wind and solar PV power in this scenario reduces the seasonal signal overall and

526 significantly decreases the percentage of RES drought hours in the summer.

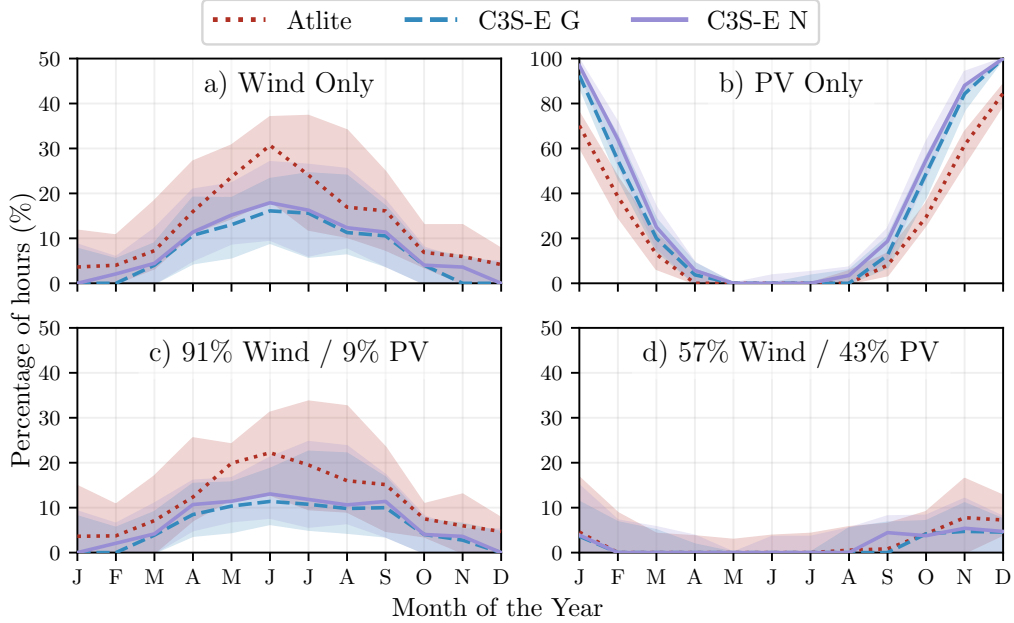


Figure 9: Percentage of hours in a month which are part of a RES drought (from 1979 to 2023) for a) Wind, b) Solar PV, c) 91W-9PV and d) 57W-43PV for Atlite (red dotted), C3S-E G (blue dashed), and C3S-E N (purple solid). The x-axis represents the month of the year, and the y-axis indicates the percentage of hours. Lines correspond to the median values and the area between the first and third quartiles is shaded. Note the different y-axis scale for b).

527 The seasonal variations observed in this study have important implica-
528 tions for energy planning. Given that energy demand peaks in winter for
529 Northern European countries, understanding these seasonal patterns is criti-
530 cal for assessing the need for conventional backup or storage solutions during
531 periods of prolonged low renewable output. The findings underscore that
532 even small differences in model assumptions leads to significant variations in
533 drought estimates, thereby affecting the reliability of the energy system dur-
534 ing critical periods. Such insights are essential for policymakers to develop
535 targeted strategies that enhance grid resilience and ensure a stable energy
536 supply throughout the year.

537 5. Conclusions

538 This study has investigated the ability of three RES datasets to repre-
539 sent RES droughts: Atlite, C3S-E G, and C3S-E N. One of the most evident
540 differences is how each dataset incorporates the specific locations of RES
541 farms. Both Atlite and C3S-E G consider the locations of wind and solar PV
542 farms, which one would expect to result in a more accurate representation
543 of RES generation. While this approach slightly improves solar PV mod-
544 els, our analysis indicates that for wind energy, the Atlite dataset performs
545 better overall, especially in its close alignment with observed data for wind
546 generation estimates. This finding suggests that, although the inclusion of
547 RES farm locations is beneficial, the accuracy of the RES dataset is more
548 strongly influenced by underlying model assumptions, such as selecting an
549 appropriate wind power curve.

550 Atlite shows the best alignment with observed data for wind generation.
551 Differences between the datasets are smaller for solar PV, with C3S-G per-
552 forming marginally better than the other two. The results show that the
553 two C3S-E datasets (C3S-E G and C3S-E N) consistently yield similar out-
554 comes, indicating that their methodological differences have minimal impact
555 in this case. This distinction is also evident in the analysis, where Atlite
556 reports higher return periods and a greater number of RES droughts, espe-
557 cially in scenarios with a balanced share of RES. Again, the results from RES
558 drought modelling rely more on the precision of the wind power curve and
559 PV panel models than on the specific locations of RES farms. Atlite's supe-
560 rior performance highlights the importance of selecting validated models for
561 assessing RES drought risks. This careful model selection can better quantify
562 risks, support effective planning, and avoid the potential underestimation of
563 capacity needs, which is essential for ensuring energy security.

564 Looking at the 57W-43PV scenario, the analysis showed a significant im-
565 provement in the management of RES droughts due to the complementary
566 nature of wind and solar PV generation. Wind and solar PV together perform
567 better in terms of reducing drought frequency and duration than either would
568 individually, largely because of the seasonal anti-correlation between the two
569 energy sources. This diversification reduces the seasonal impact on RES
570 droughts, as solar PV generation peaks in the summer and wind generation
571 is more consistent in winter. Ireland currently has a highly wind-dependent
572 energy system, but with ambitious targets for solar PV installations in the
573 coming years, the energy mix is expected to approach a balance between

574 wind and solar PV capacity. While this balanced approach offers a more
575 stable and secure energy supply by mitigating RES drought risks, it is im-
576 portant to note that having similar wind and solar PV capacities may not
577 optimise other aspects, such as annual energy production or meeting night-
578 time loads. For policymakers, these findings underscore the importance of
579 meeting these capacity targets to enhance energy security through diversifica-
580 tion. Additionally, the choice of model for RES drought assessment becomes
581 increasingly critical as more renewable capacity is integrated into the system.

582 This study has several limitations. Although ERA5 is among the best
583 reanalysis datasets for renewable energy analysis, its resolution may not cap-
584 ture local-scale phenomena, making it less reliable at the individual farm
585 level. In addition, previous studies have indicated biases in ERA5 variables
586 especially wind speed. Moreover, the methodology employs a fixed threshold
587 to define RES drought events, which is necessary for comparing the three
588 models but does not account for demand variations. Consequently, while
589 this approach enables a consistent inter-comparison, it may overlook events
590 that are most critical for power system operations.

591 Future work is planned to extend the current analysis. First, climate
592 projection data will be integrated with different energy scenarios, incorpo-
593 rating the addition of offshore wind, to better understand how climate change
594 might affect RES droughts. Second, expanding the geographic domain of the
595 study to include the rest of Europe would provide a more comprehensive un-
596 derstanding of RES droughts in an interconnected energy grid. This would
597 require extensive verification across other European countries, making it a
598 more complex but highly relevant challenge.

599 Data Availability

600 The ERA5 data can be obtained from the Climate Data Store (<https://doi.org/10.24381/cds.adbb2d47>). The C3S-E dataset is also available
601 from the Climate Data Store (<https://doi.org/10.24381/cds.4bd77450>).
602 Information on wind and solar PV farms in Ireland can be obtained from
603 the EirGrid website ([https://www.eirgrid.ie/grid/system-and-renew-
604 able-data-reports](https://www.eirgrid.ie/grid/system-and-renewable-data-reports)). The Atlite model used in this study is open-source
605 and can be found on GitHub (<https://github.com/pypsa/atlite>). The
606 data and code required to reproduce the analysis in this article will be made
607 available upon acceptance of the manuscript in a public GitHub repository.
608

609 Acknowledgments

610 The research conducted in this publication was funded by Science Foun-
611 dation Ireland and co-funding partners under grant number 21/SPP/3756
612 through the NexSys Strategic Partnership Programme.

613 References

- 614 [1] EuroStat, Renewable Energy Statistics, 2023. URL: https://ec.europa.eu/eurostat/statistics-explained/index.php?title=Renewable_energy_statistics, Accessed: 2024-11-06.
- 615
616
- 617 [2] H. C. Bloomfield, D. J. Brayshaw, L. C. Shaffrey, P. J. Coker, H. E. Thornton, Quantifying the increasing sensitivity of power systems to climate variability, *Environmental Research Letters* 11 (2016) 124025. doi:10.1088/1748-9326/11/12/124025.
- 618
619
620
- 621 [3] H. C. Bloomfield, D. J. Brayshaw, A. Troccoli, C. M. Goodess, M. De Felice, L. Dubus, P. E. Bett, Y.-M. Saint-Drenan, Quantifying the sensitivity of european power systems to energy scenarios and climate change projections, *Renewable Energy* 164 (2021) 1062–1075. doi:10.1016/j.renene.2020.09.125.
- 622
623
624
625
- 626 [4] F. Kaspar, M. Borsche, U. Pfeifroth, J. Trentmann, J. Drücke, P. Becker, A climatological assessment of balancing effects and shortfall risks of photovoltaics and wind energy in germany and europe, *Advances in Science and Research* 16 (2019) 119–128. doi:10.5194/asr-16-119-2019.
- 627
628
629
630
- 631 [5] F. Mockert, C. M. Grams, T. Brown, F. Neumann, Meteorological conditions during periods of low wind speed and insolation in Germany: The role of weather regimes, *Meteorological Applications* 30 (2023) e2141. doi:10.1002/met.2141.
- 632
633
634
- 635 [6] M. Ohba, Y. Kanno, D. Nohara, Climatology of dark doldrums in japan, *Renewable and Sustainable Energy Reviews* 155 (2022) 111927. doi:10.1016/j.rser.2021.111927.
- 636
637
- 638 [7] M. J. Mayer, B. Biró, B. Szücs, A. Aszódi, Probabilistic modeling of future electricity systems with high renewable energy penetration using
- 639

- 640 machine learning, *Applied Energy* 336 (2023) 120801. doi:10.1016/j.
641 apenergy.2023.120801.
- 642 [8] D. Raynaud, B. Hingray, B. François, J. Creutin, Energy droughts from
643 variable renewable energy sources in European climates, *Renewable*
644 *Energy* 125 (2018) 578–589. doi:https://doi.org/10.1016/j.renene
645 .2018.02.130.
- 646 [9] A. Gangopadhyay, A. K. Seshadri, N. J. Sparks, R. Toumi, The role
647 of wind-solar hybrid plants in mitigating renewable energy-droughts,
648 *Renewable Energy* 194 (2022) 926–937. doi:10.1016/j.renene.2022.
649 05.122.
- 650 [10] J. Kapica, J. Jurasz, F. A. Canales, H. Bloomfield, M. Guezgouz,
651 M. De Felice, Z. Kobus, The potential impact of climate change on
652 european renewable energy droughts, *Renewable and Sustainable En-*
653 *ergy Reviews* 189 (2024) 114011. doi:10.1016/j.rser.2023.114011.
- 654 [11] K. Z. Rinaldi, J. A. Dowling, T. H. Ruggles, K. Caldeira, N. S. Lewis,
655 Wind and Solar Resource Droughts in California Highlight the Benefits
656 of Long-Term Storage and Integration with the Western Interconnect,
657 *Environmental Science and Technology* 55 (2021) 6214–6226. doi:10.1
658 021/acs.est.0c07848.
- 659 [12] P. T. Brown, D. J. Farnham, K. Caldeira, Meteorology and climatology
660 of historical weekly wind and solar power resource droughts over western
661 North America in ERA5, *SN Applied Sciences* 3 (2021) 814. doi:10.1
662 007/s42452-021-04794-z.
- 663 [13] S. Allen, N. Otero, Standardised indices to monitor energy droughts,
664 *Renewable Energy* 217 (2023) 119206. doi:10.1016/j.renene.2023.11
665 9206.
- 666 [14] C. Bracken, N. Voisin, C. D. Burleyson, A. M. Campbell, Z. J. Hou,
667 D. Broman, Standardized benchmark of historical compound wind and
668 solar energy droughts across the Continental United States, *Renewable*
669 *Energy* 220 (2024) 119550. doi:https://doi.org/10.1016/j.renene
670 .2023.119550.
- 671 [15] H. Lei, P. Liu, Q. Cheng, H. Xu, W. Liu, Y. Zheng, X. Chen, Y. Zhou,
672 Frequency, duration, severity of energy drought and its propagation in

- hydro-wind-photovoltaic complementary systems, *Renewable Energy* (2024) 120845. doi:10.1016/j.renene.2024.120845, 2.
- [16] H. Hersbach, B. Bell, P. Berrisford, S. Hirahara, A. Horányi, J. Muñoz-Sabater, J. Nicolas, C. Peubey, R. Radu, D. Schepers, et al., The ERA5 global reanalysis, *Quarterly Journal of the Royal Meteorological Society* 146 (2020) 1999–2049. doi:10.1002/qj.3803.
- [17] L. Dubus, Y. Saint-Drenan, A. Troccoli, M. De Felice, Y. Moreau, L. Ho-Tran, C. Goodess, R. Amaro E Silva, L. Sanger, C3S Energy: A climate service for the provision of power supply and demand indicators for Europe based on the ERA5 reanalysis and ENTSO-E data, *Meteorological Applications* 30 (2023) e2145. doi:10.1002/met.2145.
- [18] F. Hofmann, J. Hampp, F. Neumann, T. Brown, J. Hörsch, Atlite: a lightweight Python package for calculating renewable power potentials and time series, *Journal of Open Source Software* 6 (2021) 3294. doi:10.21105/joss.03294.
- [19] A. Kies, B. U. Schyska, M. Bilousova, O. El Sayed, J. Jurasz, H. Stoecker, Critical review of renewable generation datasets and their implications for european power system models, *Renewable and Sustainable Energy Reviews* 152 (2021) 111614. doi:10.1016/j.rser.2021.111614.
- [20] EirGrid & SONI, System and Renewable Data Reports, 2023. URL: <https://www.eirgrid.ie/grid/system-and-renewable-data-reports>, Accessed: 2024-11-06.
- [21] E. Doddy Clarke, S. Griffin, F. McDermott, J. Monteiro Correia, C. Sweeney, Which reanalysis dataset should we use for renewable energy analysis in ireland?, *Atmosphere* 12 (2021) 624. doi:10.3390/atmos12050624.
- [22] Y.-M. Saint-Drenan, L. Wald, T. Ranchin, L. Dubus, A. Troccoli, An approach for the estimation of the aggregated photovoltaic power generated in several European countries from meteorological data, *Advances in Science and Research* 15 (2018) 51–62. doi:10.5194/asr-15-51-2018.

- 705 [23] I. Staffell, S. Pfenninger, Using bias-corrected reanalysis to simulate
706 current and future wind power output, *Energy* 114 (2016) 1224–1239.
707 doi:10.1016/j.energy.2016.08.068.
- 708 [24] Government of Ireland, Climate Action Plan 2024, Technical Report 3,
709 Department of the Environment, Climate and Communications, 2023.
710 URL: [https://www.gov.ie/pdf/?file=https://assets.gov.ie/](https://www.gov.ie/pdf/?file=https://assets.gov.ie/284675/70922dc5-1480-4c2e-830e-295afd0b5356.pdf)
711 [284675/70922dc5-1480-4c2e-830e-295afd0b5356.pdf](https://www.gov.ie/pdf/?file=https://assets.gov.ie/284675/70922dc5-1480-4c2e-830e-295afd0b5356.pdf), Accessed:
712 2024-11-06.
- 713 [25] Sustainable Energy Authority Ireland, National Energy Projections
714 2024, Technical Report, Sustainability Energy Authority of Ireland,
715 2024. URL: [https://www.seai.ie/news-and-events/news/energ](https://www.seai.ie/news-and-events/news/energy-projections-report)
716 [y-projections-report](https://www.seai.ie/news-and-events/news/energy-projections-report), Accessed: 2024-11-06.
- 717 [26] H. G. Beyer, G. Heilscher, S. Bofinger, A robust model for the mpp
718 performance of different types of pv-modules applied for the performance
719 check of grid connected systems, *Eurosun* (2004) 8.